Biochemical Engineering Journal 156 (2020) 107502

Contents lists available at ScienceDirect

Biochemical Engineering Journal

journal homepage: www.elsevier.com/locate/bej

Regular article

Potential assessment and kinetic modeling of carboxylic acids production using dairy wastewater as substrate

Milena Maciel Holanda Coelho[a], Naassom Wagner Sales Morais[a], Erlon Lopes Pereira[a], Renato Carrhá Leitão[b], André Bezerra dos Santos[a,*]

[a] Department of Hydraulic and Environmental Engineering, Federal University of Ceará, Fortaleza, Ceará, Brazil
[b] Embrapa Agroindústria Tropical. Rua Dra. Sara Mesquita, 2270, Zip: 60511-110, Fortaleza, Ceará, Brazil

HIGHLIGHTS

- Dairy wastewater (DW) is a potential substrate to produce carboxylic acids (CA).
- Kinetic modeling is a useful tool to elucidate acidogenic fermentation kinetics.
- High yield of CA (0.66 mgCA $mgCOD_A^{-1}$) was obtained from DW acidogenic fermentation.
- Models that describe an exponential phase are suitable to simulate CA production.
- Low concentrations of a medium-chain CA were achieved without e-donors addition.

ARTICLE INFO

Keywords:
Carboxylic acids
Dairy wastewater
Kinetic modeling
Anaerobic fermentation
Acidogenesis
Resource recovery

ABSTRACT

Carboxylic acids (CA) are high added-value compounds that can be produced via anaerobic fermentation by using agroindustrial residues as substrates. However, different compounds in wastewater impose uncontrolled metabolic pathways, in which the acidogenic fermentation kinetics need to be elucidated. This work aimed to assess the potential production of CA from dairy wastewater (DW) and to perform the kinetic modeling of the process. The experiments were conducted in quadruplicate batch reactors (250 mL of working volume) with inoculum from a brewery UASB at 0.61 ± 0.04 gCOD $gVSS^{-1}$. To inhibit methanogenesis, 0.05 % (v/v) chloroform was added to the reactors. The tests showed that DW is a readily fermentable substrate to acidogenic microorganisms because it presents high rates of short-chain CA formation in the first two days of the experiment. The low concentrations of medium-chain CA found indicate that fats and proteins did not function as the main carbon source for DW fermentation. The yield obtained was 0.66 mgCA $mgCOD_A^{-1}$, which corresponds to 0.83 $mgCOD_{CA}$ $mgCOD_A^{-1}$. Kinetic modeling studies have shown that mathematical models that can describe an exponential phase, such as First-order and Fitzhugh models, are suitable for simulating the production of carboxylic acids. Finally, DW seems to be a promising substrate to be investigated in the carboxylic platform.

1. Introduction

The recovery of high added-value products from agroindustrial wastes can be a sustainable and economically viable alternative to decrease the dependence on fossil fuels and implement environmentally friendly chemical processes. Carboxylic acids (CA) are among these added-value products, which can be prospected anaerobically from macromolecules fermentation by microbial consortium, usually requiring inhibition of methanogenesis and sulfetogenesis [1–3].

During acidogenic fermentation, the major CAs produced are short-chain carboxylic acids, which have up to five carbon atoms. These compounds can be used as carbon source for further processing or in the synthesis of building block chemicals, pharmaceuticals, cosmetics, materials, bioplastics, such as polyhydroxyalkanoates (PHA), and biofuels [4–6]. Compared to methane (CH_4), they are easier and safer to store and transport, besides having a higher market price [7].

In the context of agroindustry, dairy production is one of the most important components of the trade balance in developed and developing countries. World milk production reached 811 million tons in 2017 [8]. The dairy industry consumes high amounts of water and generates large volumes of wastewater, about 0.2 − 10 L of wastewater per liter of processed milk, with about 4–11 million tons of wastewater

* Corresponding author at: Department of Hydraulic and Environmental Engineering, Campus do Pici, Bloco 713. Pici. CEP, 60455-900, Fortaleza, Ceará, Brazil.
E-mail address: andre23@ufc.br (A.B. dos Santos).

https://doi.org/10.1016/j.bej.2020.107502
Received 25 September 2019; Received in revised form 16 December 2019; Accepted 20 January 2020
Available online 22 January 2020
1369-703X/

discharged annually worldwide [9,10]. Dairy wastewater (DW) is composed of suspended and dissolved solids, soluble organic components, lactose, nutrients, fats, detergent residues, and disinfectants [11,12].

Due to its high chemical oxygen demand (COD) and a high volume of wastewater generated, they may represent an interesting substrate to be investigated either on the biorefinery concept or on the carboxylic platform [11,13]. According to Atasoy et al. [14], it is estimated that, on a global scale, approximately 9.15 Mt acetic acid, 6.47 Mt propionic acid, and 5.39 Mt butyric acid could be recovered from DW, evidencing the potential of using this residue in the production of CA.

Mathematical modeling of fermentation processes is an attractive strategy for its scaling and optimization, as simulations can be applied to resource recovery treatment plants for engineering design, operation and prediction, where small process improvements can generate significant economic [15,16]. These tools are already widely studied for the complete anaerobic digestion [17–19], especially to optimize biogas production from organic wastes. However, as far as we are concerned, there are just a few studies of kinetic modeling assessing acidogenic fermentation of agroindustrial wastes, especially DW, in the perspective of the carboxylic platform.

Thus, the objective of this work was to assess the potential of CA production, perform mathematical modeling and estimate kinetic parameters that describe the hydrolysis of particulate organic matter, soluble substrate consumption and CA production under acidogenic anaerobic conditions using DW as substrate and microbial consortium as inoculum.

2. Materials and methods

2.1. Substrate and inoculum

DW was collected from a dairy industry located in the municipality of Maranguape, Ceará, Brazil. After collection, the wastewater was stored in a refrigerator at approximately 3 °C to avoid its degradation. The physicochemical characterization is shown in Table 1, whose values are in agreement with the literature [11,20].

The batch reactors used in the assays were inoculated with a sludge collected from an upflow anaerobic sludge blanket (UASB) reactor used in the treatment of brewery wastewater. Total solids (TS), total volatile solids (TVS) and total fixed solids (TFS) concentrations of the sludge were 81.0, 33.8, 47.2 g L^{-1}, respectively.

2.2. Batch tests

CA production assays were performed in quadruplicate batch reactors in borosilicate flasks with 300 mL total volume, 250 mL reaction volume and 50 mL headspace. Basal medium and pH 7.0 buffering, previously adjusted with 1 M HCl or NaOH, were performed according to the guidelines of Dams et al. [21]. The food/microorganism (F/M) ratio was 0.61 ± 0.04 gCOD $gVSS^{-1}$. To inhibit methanogenesis and promote the accumulation of the products of interest, 0.05 % (v/v) chloroform was added to batch reactors [22].

The bioreactors were sealed with butyl rubber stoppers and purged with nitrogen (N_2) for approximately 1 min to establish an anaerobic atmosphere within the flasks. They were then kept in an incubator (MA-420, Marconi LTDA, Brazil) under orbital agitation of 150 rpm and a temperature of 35 ± 0.3 °C for 7 days, which was the period required to observe the total conversion of COD added in the reactors.

Samples of 1 mL were collected from reactors on days 0, 2, 4 and 7 for COD analysis and quantification of CA in order to assess substrate conversion kinetics. At the end of the experiment, a gas sample was extracted from the headspace of the batch reactors to verify the efficiency of methanogenic inhibition and to determine the average concentrations of CH_4, hydrogen (H_2), carbon dioxide (CO_2) and hydrogen sulfide (H_2S) in the biogas.

Table 1
Physicochemical characteristics of the dairy wastewater used for batch testing.

Parameter	Representation	Average Values	Unit
Hydrogen potential	pH	5.40	–
Electric conductivity	EC	5.260	μS cm^{-1}
Color	Color	424	mgPt-Co L^{-1}
Turbidity	TB	3,760	NTU
Alkalinity	Al	223.1	mg$CaCO_3$ L^{-1}
Acidity	Ac	861.6	mgH_3COOH L^{-1}
Total Nitrogen	TN	168.4	mg-N L^{-1}
Total Kjeldahl Nitrogen	TKN	168.0	mg-N L^{-1}
Organic Nitrogen	ON	160.5	mg-N L^{-1}
Ammoniacal Nitrogen	AmN	9.4	mg-N L^{-1}
Total Oxygen Chemical Demand	COD_T	17,629	mgO_2 L^{-1}
Soluble Chemical Oxygen Demand	COD_S	12,365	mgO_2 L^{-1}
Particulate Chemical Oxygen Demand	COD_P	5,264	mgO_2 L^{-1}
Total Biochemical Oxygen Demand	$BOD_{5T}^{20°C}$	11,875	mgO_2 L^{-1}
Soluble Biochemical Oxygen Demand	$BOD_{5S}^{20°C}$	10,000	mgO_2 L^{-1}
Particulate Biochemical Oxygen Demand	$BOD_{5P}^{20°C}$	1,875	mgO_2 L^{-1}
Total Phosphorous	TP	105.4	mg-P L^{-1}
Orthophosphate	PO_4^{-3}	52.9	mg-P-PO_4^{3-} L^{-1}
Sulfate	SO_4^{2-}	43.9	mg L^{-1}
Fluoride	F^-	36.3	mg L^{-1}
Chloride	Cl^-	2984.8	mg L^{-1}
Total Solids	TS	18,263	mg L^{-1}
Total Volatile Solids	TVS	12,292	mg L^{-1}
Total Fixed Solids	TFS	5,971	mg L^{-1}
Total Dissolved Solids	TDS	15,679	mg L^{-1}
Volatile Dissolved Solids	VDS	9,796	mg L^{-1}
Fixed Dissolved Solids	FDS	5,883	mg L^{-1}
Total Suspended Solids	TSS	2,584	mg L^{-1}
Volatile Suspended Solids	VSS	2,496	mg L^{-1}
Fixed Suspended Solids	FSS	88	mg L^{-1}
Hexane Soluble Substances	O.G	94.6	mg L^{-1}

2.3. Analytical methods

Physicochemical characterization analyses were performed according to Standard Methods for the Examination of Water and Wastewater [23].

Biogas composition was analyzed by gas chromatography with dielectric barrier ionization discharge (GC BID-2010 Plus, Shimadzu Corporation, Japan) equipped with a GS-GASPRO column (60 m x 0.32 mm) (Agilent Technologies Inc., USA). The oven, injector and detector temperatures were 250, 50 and 100 °C, respectively. Helium gas (White Martins LTDA, Brazil) was used as a carrier gas in a 2 mL min^{-1} flow, and the run time of the method was 9 min. Biogas quantification was performed by recording the accumulated pressure in each batch reactor using a gauge pressure transmitter (Warme LTDA, Brazil).

Acetic (HAc), propionic (HPr), butyric (HBu), isovaleric (i-HVa), valeric (HVa) and caproic (HCa) acids concentrations were determined by high performance liquid chromatography (HPLC) using HPLC LC-20A chromatograph (Prominence, Shimadzu Corporation, Japan) equipped with Aminex HPX-87H (300 mm x 7.8 mm) column (Bio-Rad, USA) at 65 °C with sulfuric acid (H_2SO_4) 5 mM in deionized water as eluent (0.6 mL min^{-1} isocratic flow) and refractive index detector (RID-10A, Shimadzu Corporation, Japan). For chromatographic and soluble COD analyses, the samples were filtered through a 0.45 μm pore glass fiber membrane (EMD Millipore, USA).

2.4. Mass balance and yields

A mass balance of the system was performed in terms of COD using Eq. (1–10) expressed in Table 2. The concentrations of CA were

Table 2
Equations used for mass balance calculations.

Equation	Mass balance equation
1	$COD_P = COD_T - COD_S$
2	$COD_A = COD_T - COD_{CA(t0)}$
3	$COD_C = COD_A - COD_{Bio(tf)}$
4	$COD_{Bio} = COD_S - COD_{CA}$
5	$COD_{CA} = COD_{CA(tf)} - COD_{CA(t0)}$
6	$COD_{VSS} = COD_A - COD_{CA} - COD_{Bio(tf)} - COD_{BG}$
7	$Y_C = \frac{COD_C}{COD_A}$
8	$Y1_{CA} = \frac{COD_{CA}}{COD_A}$
9	$Y_{SSV} = \frac{COD_{VSS}}{COD_A}$
10	$Mass\ Balance = \frac{COD_S + COD_{BG} + COD_{VSS}}{COD_T}$

Legend: COD_P: particulate COD added in the batch reactor. COD_T: total COD added in the batch reactor. COD_S: soluble COD added in the batch reactor. COD_A: fraction of the total COD available to be bioconverted to CA or directed to cell growth and biogas formation, corresponds to the total COD fraction applied at the beginning of the experiment that is not in the form of CA. $COD_{CA(t0)}$: fraction of soluble COD in the form of CA at the beginning of the batch. COD_C: COD directed to the production of CA, cell growth and biogas formation. $COD_{Bio(tf)}$: soluble COD fraction not related to CA at the end of the incubation period. COD_{Bio}: fraction of COD soluble not referring to CA. COD_{CA}: mass of CA formed during the incubation period. $COD_{CA(Tf)}$: mass of CA at the end of the incubation period. COD_{VSS}: COD directed to cell growth. COD_{BG}: COD removed by biogas production (methane or hydrogen). Y_C: stoichiometric coefficient of total yield of converted COD. $Y1_{CA}$: stoichiometric coefficient of COD yield converted to CA. Y_{VSS}: stoichiometric coefficient of cell growth yield. Units in mgCOD.

multiplied by the reaction volume in the bioreactor on the day of collection to obtain the mass of CA. The concentration of organic matter (COD in the form of acids) of each acid was obtained by the following conversion factors: 1 mgHAc = 1.07 mgCOD. 1 mgHPr = 1.51 mgCOD. 1 mgHBu = 1.82 mgCOD. 1 mgi-HVa = 2.04 mgCOD. 1 mgHVa = 2.04 mgCOD. 1 mgHCa = 2.21 mgCOD [24].

The yield, selectivity, and productivity of CA were calculated according to Eqs. (11), (12) and (13), respectively.

$$Y2_{CA} = \frac{M_{TCA}}{COD_A} \quad (11)$$

$$\text{Selectivity} = \frac{M_{CA}}{M_{TCA}} x\ 100 \quad (12)$$

$$\text{Productivity} = \frac{C_{CA1D} - C_{CAB}}{Time} \quad (13)$$

where: $Y2_{CA}$: CA production in relation to the available COD (mg_{CA} $mgCOD_A^{-1}$); M_{TCA}: total mass of CA formed during the incubation period (mg_{CA}); COD_A: total COD mass fraction available to be converted at the beginning of the batch (mgCOD); Selectivity: percentage of each CA formed in relation to the total acids produced (%); M_{CA}: mass of CA formed during the incubation period (mg_{CA}); Productivity: quantity of CA present per working volume and per time (mg_{CA} L^{-1} d^{-1}); C_{CA1D}: CA concentration at one day of collection (mg_{CA} L^{-1}); C_{CAB}: CA concentration at the beginning of the batch (day zero) (mg_{CA} L^{-1}); and Time: unit of time (d).

2.5. Model fitting

The equations of the kinetic models selected to describe the hydrolysis process of particulate organic matter, soluble substrate consumption, and CA production in terms of COD and individual CA production are presented in Table 3.

A nonlinear least-squares regression analysis was performed using the Microsoft Office Excel 2019 Solver tool to estimate the parameters

Table 3
Selected models to describe the conversion of organic matter (hydrolysis, soluble substrate consumption and production of carboxylic acids – in terms of COD and individual acids).

Kinetic Model	Equation of the Kinetic Model
Hydrolysis	
First-order	$C_t = C_0\ exp(-kt)$
First-order with Residual	$C_t = C_r + (C_0 - C_r)\ exp(-kt)$
Consumption of Soluble Substrate (Biodegradable COD)	
First-order	$C_t = C_0 exp(-kt)$
First-order with Residual	$C_t = C_r + (C_0 - C_r) exp(-kt)$
Logistic	$C_t = \frac{C_0 + X_0}{1 + \left(X_0/C_0\right) exp[K_L (C_0 + X_0) t]}$
Monod with Growth	$C_t = exp\left(\frac{(C_0 + X_0 + K_S)\ln\left(\frac{X}{X_0}\right) - (C_0 + X_0)\mu_{m\acute{a}x} t + K_S \ln(C_0)}{K_S}\right)$
Production of Carboxylic Acids	
First-order	$CA_t = CA_f\ [1 - exp(-k_{CA} t)]$
Second-order	$CA_t = \frac{k_{CA}''(CA_f)^2 t}{1 + k_{CA}''(CA_f) t}$
Fitzhugh	$CA_t = CA_f\ [1 - exp(-k_{CA} t)^n]$
Cone	$CA_t = \frac{CA_f}{1 + (k_{CA} t)^{-n}}$
BPK	$CA_t = CA_f \left\{1 - exp\left[(m-1)\left(\frac{t}{t_0}\right)^{1/m}\right]\right\}$ $\mu_m = \frac{CA_f exp(m)(1-m)}{e \cdot m \cdot t_0}$ $\quad k_{CA} = \frac{exp(m)(1-m)}{e \cdot m \cdot t_0}$
Monomolecular	$CA_t = CA_f\ \{1 - exp\ [-k_{CA}(t - \lambda)]\}$
Modified Gompertz	$CA_t = CA_f exp\left\{-exp\left[\frac{\mu_m e}{CA_f}(\lambda - t) + 1\right]\right\}$
Logistic	$CA_t = \frac{CA_f}{1 + exp\left[\frac{4\mu_m(\lambda - t)}{CA_f} + 2\right]}$

Legend: C_t: concentration of organic matter over time; C_0: initial organic matter concentration; k: velocity constant (k_H: hydrolysis rate constant/k_B: soluble substrate degradation rate constant); C_r: residual organic matter concentration; X_0: initial biomass concentration; X: final biomass concentration; k_L: Logistic model constant; K_S: saturation constant/Monod constant; μ_{max}: maximum microbial growth rate; CA_t: CA concentration over time; CA_f: final concentration of CA; k_{CA}: first-order CA production rate constant, k_{CA}": second-order CA production rate constant, t: digestion time, n: shape constant; m: constant of the BPK model; e: Euler number; λ: lag phase time; μ_m: maximum CA productivity.

of the selected kinetic models. This method adjusts the values of the model variables in order to minimize the sum of the squares of the differences between predicted and measured values. Data obtained from kinetic modeling were applied to plot the curves of each process using Origin software version 8.1 (OriginLab Corporation, Northampton, MA, USA).

2.6. Statistical analyses

The selection of the model that best describes each organic matter conversion process was performed using the determination coefficient (R^2) and the following error functions: root mean square error (RMSE); normalized root mean square error (NRMSE) and Akaike Information Criterion (AIC) [25,26].

$$RMSE = \sqrt{\frac{\sum_i (Y_{i,exp} - Y_{i,est})^2}{n}} \quad (14)$$

$$NRMSE = \left[\frac{RMSE}{(Y_{max} - Y_{min})}\right] x\ 100 \quad (15)$$

$$AIC = N.\ ln\left(\frac{SS}{N}\right) + 2k \quad (16)$$

Table 4
Mass balance of fermentative assays using dairy wastewater as substrate.

[a]Time	[b]COD_T	[b]COD_P	[b]COD_S	[b]COD_{CA}	[b]COD_{BIO}	[b]COD_{BG}
0	700.7 ± 0.0	250.0 ± 0.0	450.7 ± 0.0	9.0 ± 0.0	441.7 ± 0.0	
2	660.6 ± 27.1	133.3 ± 38.3	527.3 ± 39.7	440.6 ± 35.2	86.6 ± 23.9	
4	657.6 ± 5.2	96.6 ± 14.3	561.0 ± 18.8	525.8 ± 5.9	35.2 ± 16.2	
7	654.4 ± 10.3	60.7 ± 11.3	593.7 ± 9.8	586.5 ± 6.4	7.2 ± 4.9	0.0 ± 0.0
[b]COD_A	[b]COD_{CA}	[b]COD_C	[b]COD_{VSS}	[c]Y_C	[d]$Y1_{CA}$	[e]Y_{VSS}
691.7 ± 0.0	577.5 ± 6.4	684.5 ± 4.9	107.0 ± 9.8	0.99 ± 0.01	0.83 ± 0.01	0.15 ± 0.01

Legend: a. Time in day (d); b. Mass in mgCOD; c. Y_C: Yield of converted COD ($mgCOD_C\ mgCOD_A^{-1}$); d. $Y1_{CA}$: COD yield converted to carboxylic acids ($mgCOD_{CAf}\ mgCOD_A^{-1}$); e. Y_{VSS}: yield of COD converted to biomass ($mgCOD_{VSS}\ mgCOD_A^{-1}$).

where: n is the number of experimental data points (observations); Y_{max} and Y_{min} are the observed maximum and minimum values for the evaluated response variable, respectively; AIC is the Akaike Information Criterion (dimensionless); N is the number of observations of experimental data; SS is the square sum of the residuals and k is the number of model parameters.

3. Results and discussions

3.1. Mass balance

The mass balance showed that most of the initial substrate COD that was available to the microorganisms (691.97 ± 0.00 mgCOD $-COD_A$) was converted to CA (83 ± 1 %), while the remaining COD was either directed to new cell formation (15 ± 1 %) or remained available for microbial conversion or other non-detected products (1 ± 1 %) (Table 4). Therefore, 99 ± 1 % of the total applied COD was biologically transformed in CA and new cells, representing a mass of 684.5 ± 4.9 mgCOD (COD_C), and demonstrating a high biodegradability of the DW, as reported by Silva et al. [27].

The yield of CA formation in relation to the available COD ($Y1_{CA}$), as well as the biomass formed in relation to the converted COD (Y_{VSS}), were 0.83 ± 0.01 $mgCOD_{CA}\ mgCOD_A^{-1}$ and 0.15 ± 0.01 $mgCOD_{VSS}\ mgCOD_A^{-1}$, respectively, resulting in a converted COD yield (Y_C) of 0.99 ± 0.01 $mgCOD_C\ mgCOD_A^{-1}$ (Table 4). These coefficients are essential to the design of biochemical reactors, to determine if the process would be economically viable and to help the process optimization in terms of efficiency and costs [28].

The biogas formed was mainly composed of CO_2 followed by traces of H_2. The concentrations of CH_4 and H_2S were below the quantification limit of the chromatographic method. Therefore, COD removal by biogas production was considered null (COD_{BG} = 0). Thus, it can be inferred that the inhibition of methanogenic archaea with 0.05 % (v/v) chloroform was efficient. Chloroform is a nonspecific inhibitor capable of inhibiting the methyl-coenzyme M reductase in methanogenic archaea, and may also interfere with the metabolism of homoacetogenic and sulfate-reducing bacteria (SRB) [29].

About 577.5 ± 6.4 mg of COD was produced in terms of CA considering the available organic matter that was applied (COD_A), from which 305.3 ± 7.4 mgCOD was directed to HAc production, 176.9 ± 3.1 to HPr, 48.0 ± 1.4 to HBu, 26.8 ± 1.0 to i-HVa, 8.9 ± 0.4 to HVa and 11.7 ± 0.2 to HCa. Therefore, 53 ± 1 % of the converted COD was directed to the formation of HAc; 31 ± 1 % to HPr; 8 ± 1 % to HBu; 5 ± 1 % to i-HVa; 2 ± 1 % to HVa and 2 ± 1 % to HCa.

In this sense, 92 % of the converted COD was to the production of HAc, HPr, and HBu. The result obtained is consistent with the literature, as HAc, HPr and HBu are the main CA synthesized during acidogenic fermentation of organic waste using microbial consortium, and the distributions of the main soluble products reflect the predominant metabolic pathways in the bioreactor [30,7].

About 2 ± 1 % of the organic matter converted to CA was directed to the production of HCa, which differs from the others because it is a medium-chain carboxylic acid (MCCA) and has a higher added-value in the industry. HCa can be biologically formed by an elongation process, which takes place via the reverse β-oxidation pathway, in the presence of an electron donor such as lactic acid (HLa), ethanol (EtOH) or H_2 [31,32].

At the beginning of the experiment, 124.5 and 13.1 mgCOD of HLa and EtOH were detected, respectively, which may have been directed to HAc and other acids production or even to elongation processes. Other short-chain acids such as HBu, i-HVa, and HVa can also be produced by chain elongation, as this is a process of sequentially adding two carbons to an even or odd chain CA [32]. After the beginning of the experiment, no concentrations of HLa and EtOH were detected, indicating that these compounds were consumed.

In literature, DW is commonly used in studies aimed at H_2 production, since lactose is a potential substrate [33]. On the other hand, reports of CA production from DW are scarce. Some studies have used cheese whey, a liquid by-product of the dairy industry – made up of lactose, protein, and lipids – to evaluate CA production.

For instance, Silva et al. [27] studied the acidification potential (i.e. the ratio between acid COD produced and the total applied COD) of a variety of organic residues, including cheese whey. They used batch reactors (working volume of 230 mL) with sewage sludge as inoculum, F/M ratio of 4 gCOD $gVSS^{-1}$, temperature of 37 °C and 2-bromoethanesulfonic acid (BES) to inhibit methanogenesis. The results indicated that cheese whey was a highly fermentable substrate, with an acidification degree of 39.8 ± 1.3 %, and 51.6 ± 3.8 % of the soluble COD was CA on the last day of the experiment (30th day).

On the other hand, in the current investigation, about 98 % ± 0.81 of the soluble COD corresponded to CA on the seventh day of the experiment, indicating that in Silva et al. [27] other metabolites, such as alcohols, may have been produced over the experimental time, contributing to the reduction of the CA formed in relation to the soluble COD available. Therefore, depending on the type of substrate and conditions applied, the COD available can be transformed into acids in the first days of testing as reported elsewhere [34,35].

3.2. Productivity, selectivity, and yield of carboxylic acids

The maximum productivity rate (μ_m) of CA occurred on the second day of the experiment for all acids (Table 5), and the highest values achieved were for HAc (μ_m = 420.4 ± 34.5 mg $L^{-1}\ d^{-1}$) and HPr (μ_m = 202.8 ± 13.3 mg $L^{-1}\ d^{-1}$). The average of μ_m was 999.65 ± 597.35 mg $L^{-1}\ d^{-1}$ and the total yield of CA ($Y2_{CA}$) was 0.66 mgCA $mgCOD_A^{-1}$, which corresponds to 0.83 $mgCOD_{CA}\ mgCOD_A^{-1}$ ($Y1_{CA}$).

The maximum productivity of HAc and HBu occurred on the second day (Table 5), suggesting that the addition of electron donors on this time of fermentation could favor the chain elongation process for HCa production in processes with similar kinetics, as HAc and HBu are the main electron acceptors to the chain elongation for HCa [31,32]. Since there was no addition of electron donors for HCa production, the results of using DW as a substrate for acidogenic fermentation and chain elongation studies are promising.

Table 5
Maximum productivity rate, selectivity and yield of carboxylic acids from the fermentative assays using dairy wastewater as substrate.

Parameter	HAc	HPr	HBu	i-HVa	HVa	HCa
[a]Maximum productivity rate	420.4 ± 34.5	202.8 ± 13.3	31.8 ± 6.6	15.0 ± 1.3	4.9 ± 0.6	4.4 ± 1.28
[b]Selectivity	63 ± 0.8	26 ± 0.6	6 ± 0.2	3 ± 0.1	1 ± 0.0	1 ± 0.0
[c]Yield	0.4 ± 0.02	0.17 ± 0.01	0.04 ± 0.01	0.02 ± 0.01	0.01 ± 0.01	0.01 ± 0.01

Legend: a. Maximum productivity rate (μ_m) of each acid produced (mg L^{-1} d^{-1}); b. Percentage of each acid formed in relation to the total acids produced (%); c. Each acid yield in relation to the applied COD (mgCA mgCOD_A^{-1}).

In addition, the highest productivity and selectivity found for HAc are consistent with the studies of Chartrain and Zeikus [36], who reported that acetate corresponded to about 70 % of the intermediate metabolites produced from anaerobic lactose digestion. The substrate composition used in CA synthesis can influence both the amount produced and the distribution of acids and is one of the factors determining the choice of bioprocess operating parameters [37].

As the ranges are well-reported in the literature [38], it is known that DW is composed mainly of lactose (250 − 930 mg L^{-1}), but fats (35 − 500 mg L^{-1}) and proteins (210 − 560 mg L^{-1}) are also part of its composition, likely being used as carbon sources during the fermentation process. Carbohydrates such as lactose are converted to glucose by enzymes, and most of the anaerobic bacteria use the Embden-Meyerhof-Parnas (EMP) glycolytic pathway to metabolize lactose [38].

Lactose hydrolysis involves sequential reactions with intermediate saccharides by β-galactosidase, which catalyzes lactose hydrolysis to galactose and glucose. Pyruvate produced from the EMP pathway is the main control point for fermentation, as it can be converted by acidogenic bacteria into a wide variety of metabolites such as HAc, HPr, HBu, alcohols (EtOH, propanol, and butanol), H_2 and CO_2. Subsequently, HPr, HBu, alcohols, and CO_2 are converted to HAc by proton reducing acetogenic pathways or by the homoacetogenic pathway [7,38,39].

In literature, it is already well established that HAc, HPr, and HBu are the acids mostly produced in carbohydrate fermentation [37]. Kisaalita et al. [40] studied the acidogenic fermentation of lactose in continuous flow reactor (1.5 L) using anaerobic sewage sludge at mesophilic temperature, pH 6.5 and stirring at 400 rpm. The authors concluded that HAc and HBu were the main products formed, and EtOH, HPr and HCa were formed in lower concentrations.

Although the carbohydrate fraction was not quantified in the physicochemical characterization of DW (Table 1), it is possible to infer from the CA profile generated that, carbohydrates, especially lactose, were the carbon source mostly used by the acidogenic microorganisms. In addition, lactose degradation provides the highest formation of HAc and HBu, according to the studies by Kisaalita et al. [38]. However, HPr was produced in larger proportions than HBu in DW fermentation, indicating that differences in individual CA depend on the complexity and heterogeneity of substrates (such as protein and lipid content) and the different operational parameters applied, which may activate or inactivate specific metabolic pathways [5,37].

Concentrations of oils and greases (94.6 mg L^{-1}) and total nitrogen (168.3 mg-N L^{-1}) in the DW physicochemical characterization (Table 1) indicate, respectively, the presence of lipids and proteins (such as casein) in milk. Lipids and proteins are considered less biodegradable than carbohydrates. In slow lipid metabolization, long-chain fatty acids (LCFA) are produced which can adhere to the bacterial cell wall and cause metabolic inhibition. Proteins, by presenting tertiary and quaternary three-dimensional structures, make proteases action more difficult. For these reasons, lipid and protein hydrolyses are usually considered the limiting step of acidogenic fermentation [37,41]. Because it is a wastewater from industrial processes that involve heat exchange [38], protein hydrolysis was not a limiting factor of acidogenic fermentation, since it is likely that proteins have gone through a denaturation process, which compromises its three-dimensional structure.

In addition, satisfactory i-HVa, HVa, and HCa production are related to protein fermentation, since the acidogenesis of non-proteinaceous substrates showed low yields of these CAs [42,43]. The low concentrations of these acids, as well as the short lag time in relation to CA production (section 3.4), indicate that in our case fats and proteins did not function as the main carbon source for DW fermentation, which is in agreement with other investigations [35,41].

Bengtsson et al. [44] studied the acidogenic fermentation of cheese whey in batch reactors (1.0 L) with acidogenic anaerobic sludge, mesophilic temperature (37 °C), pH 6.0 and reaction time of 17–57 days until CA stabilization production was achieved. The authors obtained higher selectivity of HAc (43 %), HPr (15 %) and HBu (42 %) and yield of 0.60 gCA $gCOD_A^{-1}$. The acids i-HVa, HVa and HCa acids were produced with low selectivity, and EtOH was not detected. The results were similar to the current experiments performed with DW since the yield obtained was 0.66 gCA $gCOD_A^{-1}$.

3.3. Kinetic modeling of hydrolysis and soluble substrate consumption

There was a continuous hydrolysis process of the particulate COD, as this fraction decreased in the system. Thus, soluble and biodegradable COD represented by carbohydrates, proteins and lipids and other soluble organic compounds, became available gradually. Simultaneously, the portion of biodegradable COD (available for conversion) decreased progressively and continuously, as shown in Fig. 1A, indicating that the consumption of this COD fraction occurred faster when compared to the COD fraction generated from the hydrolytic process. These results can be confirmed from the analysis of the estimated kinetic parameters from the mathematical COD conversion modeling (Table 6).

Soluble substrate degradation rate constant (k_B = 0.86 ± 0.31 d^{-1}) was higher than the hydrolysis rate constant (k_H = 0.47 ± 0.50 d^{-1}), according to First-order with residual model (Table 6). Since $k_B > k_H$, the biodegradable COD consumption rate was higher than the degradation rate of the particulate COD fraction (Figs. 1B and 1C). The soluble substrate decay is high, between the first and the second day (Fig. 1C), while the decay of particulate organic matter is slower considering the same period (Fig. 1B). The higher concentration of biodegradable COD available on the first day (1.77 gCOD L^{-1}) compared to particulate COD concentration (1.00 gCOD L^{-1}) may have contributed to this [45].

The First-order kinetic model with residual was the model that best fit not only the hydrolysis curve of particulate organic matter (Fig. 1B), with a high coefficient of determination (R^2 = 0.995) and lower AIC value (-29.062), but also the curve formed by the consumption of soluble substrate (Fig. 1C), with high R^2 (0.999) and lower AIC values (-25.950). This model, when considering the concentration of residual soluble organic matter (C_r) in its equation, may provide a better fit than the First-order model. Nevertheless, the First-order kinetic model (without residual) was also quite suitable for the mathematical simulation of both processes.

Logistic and Monod with growth models were also used to describe the consumption of soluble substrate and presented the least satisfactory adjustment performance (Table 6). The Logistic model is increasingly applied in the study of fermentative processes [18], being able to

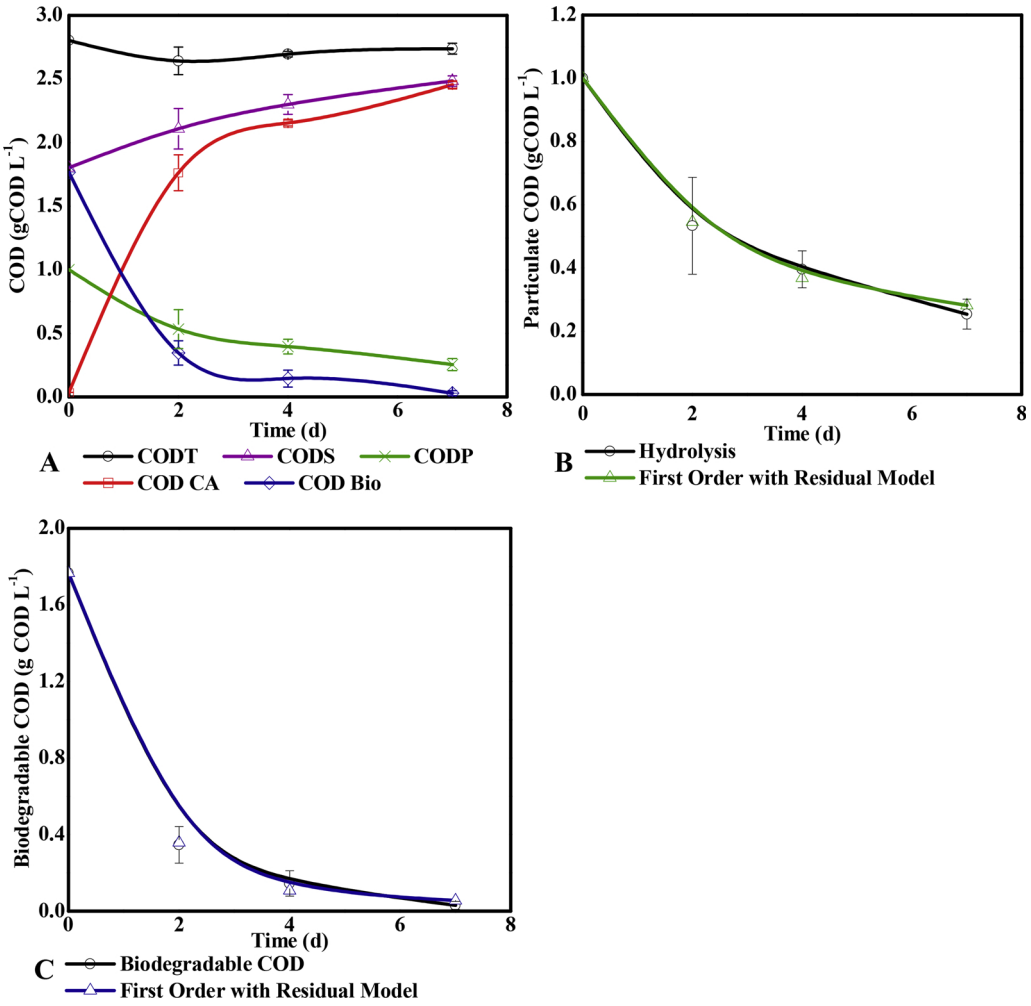

Fig. 1. Organic matter concentration profiles (A), Kinetic modeling of hydrolysis of particulate COD (B) and Kinetic modeling of the biodegradable COD (C), during the fermentative tests using dairy wastewater as substrate.

Table 6
Parameters estimated from hydrolysis kinetic modeling and soluble substrate consumption from fermentative assay using dairy wastewater as substrate.

Model	Parameter	Value	Model	Parameter	Value
Hydrolysis					
First-order	k_H (d^{-1})	0.24 ± 0.14	First-order with	C_r (gCOD L^{-1})	0.25 ± 0.05
	R^2	0.962	Residual	k_H (d^{-1})	0.47 ± 0.50
	RMSE	0.055		R^2	0.995
	NRMSE	7.363		RMSE	0.021
	AIC	−21.215		NRMSE	2.761
				AIC	−29.062
Consumption of Soluble Substrate					
First-order	k_B (d^{-1})	0.77 ± 0.19	First-order with	C_r (gCOD L^{-1})	0.05 ± 0.03
	R^2	0.997	residual	k_B (d^{-1})	0.86 ± 0.17
	RMSE	0.037		R^2	0.999
	NRMSE	2.135		RMSE	0.024
	AIC	−24.359		NRMSE	1.363
				AIC	−25.950
Monod with growth	K_S (gCOD L^{-1})	5.86 ± 2.18	Logistic	k_L (L $gCOD^{-1}$ d^{-1})	0.66 ± 0.11
	X (gSSV L^{-1})	4.70 ± 0.00		k_B (d^{-1})	0.14 ± 0.02
	$\mu_{máx}$ (d^{-1})	0.70 ± 0.31		R^2	0.996
	k_L (L $gCOD^{-1}$ d^{-1})	0.12 ± 0.02		RMSE	0.044
	k_B (d^{-1})	0.56 ± 0.09		NRMSE	2.549
	R^2	0.997		AIC	−22.940
	RMSE	0.037			
	NRMSE	2.133			
	AIC	−20.366			

Legend: k_H: hydrolysis rate constant; k_B: soluble substrate degradation rate constant; C_r: residual COD concentration; K_S: saturation constant/Monod constant; X: final biomass concentration; μ_{max}: maximum microbial growth rate; k_L: Logistic model constant; R^2: coefficient of determination; RMSE: roof mean square error; NRMSE: normalized roof mean square error; AIC: Akaike Information Criteria.

Table 7
Parameters estimated from the kinetic modeling of COD production for carboxylic acids from fermentative assay using dairy wastewater as substrate.

Model	Parameter	Value	Model	Parameter	Value
First-order	k_{CA} (d^{-1})	0.60 ± 0.06	Second-order	k_{CA}"(L $gCOD^{-1}$ d^{-1})	0.65 ± 0.11
	R^2	0.997		R^2	0.985
	RMSE	0.052		RMSE	0.117
	NRMSE	2.142		NRMSE	4.819
	AIC	−21.683		AIC	−15.197
Fitzhugh	k_{CA} (d^{-1})	0.47 ± 0.09	Cone	k_{CA} (d^{-1})	0.81 ± 0.17
	n	0.69 ± 0.33		n	1.91 ± 0.30
	R^2	0.998		R^2	0.996
	RMSE	0.041		RMSE	0.057
	NRMSE	1.699		NRMSE	2.343
	AIC	−21.539		AIC	−18.967
Monomolecular	k_{CA} (d^{-1})	0.60 ± 0.06	Modified Gompertz	μ_m ($gCOD\ L^{-1}\ d^{-1}$)	0.98 ± 0.11
	λ (d)	0.00 ± 0.00		λ (d)	0.16 ± 0.02
	R^2	0.997		R^2	0.987
	RMSE	0.052		RMSE	0.109
	NRMSE	2.142		NRMSE	4.491
	AIC	−19.683		AIC	−13.762
Logistic	μ_m ($gCOD\ L^{-1}\ d^{-1}$)	1.29 ± 0.18	BPK	m	0.47 ± 0.07
	λ (d)	0.62 ± 0.05		t_0 (d)	1.83 ± 0.28
	R^2	0.976		μ_m ($gCOD\ L^{-1}\ d^{-1}$)	0.88 ± 0.04
	RMSE	0.145		k_{CA} (d^{-1})	0.36 ± 0.02
	NRMSE	5.983		R^2	0.997
	AIC	−11.466		RMSE	0.052
				NRMSE	2.142
				AIC	−19.683

Legend: k_{CA}: first-order CA production rate constant, k_{CA}": second-order CA production rate constant; n: form constant; λ: lag phase time; μ_m: maximum CA productivity; m: constant of the BPK model; R^2: coefficient of determination; RMSE: roof mean square error; NRMSE: normalized roof mean square error; AIC: Akaike Information Criteria.

estimate a constant k_L, defined as the ratio between the maximum growth rate (μ_{max}) and the Monod saturation constant (K_S), therefore $k_L = \mu_{max}/K_S$. The higher μ_{max}, the higher the k_L and the higher the affinity of the microorganisms for the substrate. Through mathematical relationships, k_L (0.66 ± 0.11 L $gCOD^{-1}$ d^{-1}) was obtained from the data estimated by the growing Monod model and, through it, k_B (0.14 ± 0.02 d^{-1}).

Mathematical modeling using the growing Monod kinetic model presented the least satisfactory performance among the models tested for soluble substrate consumption. The Monod constant K_S obtained was 5.86 ± 2.18 gCOD L^{-1}.

It is noteworthy that the final biomass concentration value estimated by the model (X = 4.70 ± 0.00 gVSS L^{-1}) was the same as the initial biomass concentration (X_0) added in the assays, indicating that there was no cell growth. Nevertheless, 15 ± 1 % of the converted organic matter was directed to biomass production (Table 4, Section 3.1), which allows inferring low cell growth, as expected for anaerobic systems.

Some factors may have influenced the fit, given this inconsistency, as the Monod model is highly accurate for pure cultures and simple substrates, but fails to satisfactorily describe substrate consumption for heterogeneous cultures. In addition, its use is limited when cultivation conditions change rapidly or when there are low substrate concentrations [28,46].

3.4. Kinetic modeling of carboxylic acids production

Among the models tested to describe CA production in terms of COD, the First-order model presented the best fit to CA production data, with satisfactory R^2 (0.997) and lower AIC values (-21.683) compared to the other models, allowing to estimate the CA production rate constant (k_{CA}) of 0.60 ± 0.06 d^{-1}. It is noticed that the production of CA in terms of COD from DW follows first-order kinetics [45], as evidenced by the lower values of the error functions of the First-order model in relation to that of Second-order model (Table 7).

The COD production curve in terms of COD (Fig. 2) resembles a reverse L-shape, which characterizes a high COD productivity in the first days of incubation and an absence or short lag period relative to the production of acids [19]. At the end of the seven days of the experiment, 2.42 ± 0.03 gCOD L^{-1} of CA were formed, and 64 % of this concentration was produced in the first 48 h. Probably, the kinetics of acid production from DW resembles the kinetics of microbial growth, conventionally described by the Monod model (1942), the enzymatic kinetics of Michaelis-Menten (1902) and the kinetics of CH_4 production in anaerobic reactors, whose curves are hyperbolic functions and have an exponential phase [19,47]. Therefore, the First-order, Fitzhugh, and Cone models may be suitable for this purpose.

Three models (Monomolecular, Modified Gompertz and Logistic) provided as output lag phases (λ) lower than one day, and one of them

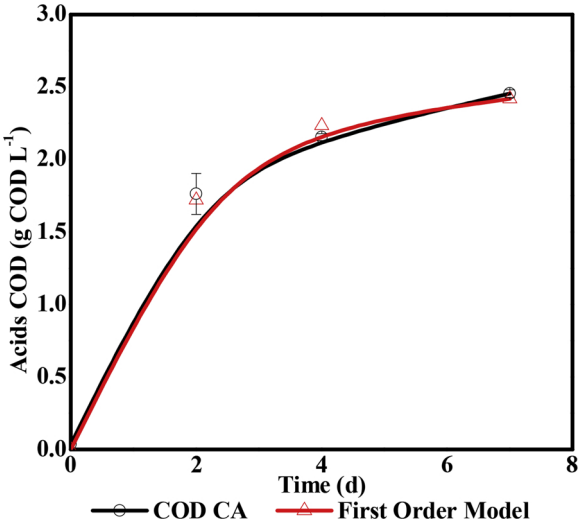

Fig. 2. Kinetic modeling of COD production in the form of carboxylic acids (First-order model) from the fermentative assays using dairy wastewater as substrate.

Table 8
Parameters estimated from the kinetic modeling of the production of carboxylic acids from the fermentative assays using dairy wastewater as substrate.

Model	Parameter	HAc	HPr	HBu	i-HVa		HVa	HCa
First-order	k_{CA} (d^{-1})	0.611	0.800	0.411	0.453		0.401	0.321
	R^2	0.999	0.988	0.990	0.990		0.993	0.969
	RMSE	0.011	0.021	0.004	0.002		0.001	0.001
	NRMSE	0.874	4.254	3.745	3.940		3.209	6.542
	AIC	−34.242	−28.985	−41.908	−47.070		−57.522	−50.255
Fitzhugh	k_{CA} (d^{-1})	0.587	0.292	0.409	0.748		0.478	0.544
	n	0.936	0.244	0.993	2.397		1.307	2.316
	R^2	0.999	0.996	0.990	0.999		0.994	0.993
	RMSE	0.010	0.012	0.004	0.000		0.001	0.001
	NRMSE	0.850	2.391	3.744	0.665		2.807	3.020
	AIC	−32.464	−31.595	−39.908	−59.304		−56.592	−54.438
Monomolecular	k_{CA} (d^{-1})	0.611	0.800	0.411	0.457		0.405	0.328
	λ (d)	0.000	0.000	0.000	0.024		0.024	0.079
	R^2	0.999	0.988	0.990	0.990		0.993	0.971
	RMSE	0.011	0.021	0.004	0.002		0.001	0.001
	NRMSE	0.874	4.254	3.745	3.899		3.207	6.397
	AIC	−32.242	−26.985	−39.908	−45.153		−55.526	−48.434
Logistic	μ_m (g L^{-1} d^{-1})	0.764	0.419	0.027	0.019		0.005	0.005
	λ (d)	0.838	0.955	0.023	0.535		0.154	0.508
	R^2	0.985	0.977	0.937	0.985		0.957	0.981
	RMSE	0.059	0.029	0.010	0.003		0.001	0.001
	NRMSE	4.768	5.979	9.232	4.719		7.742	5.193
	AIC	−18.665	−24.262	−32.688	−43.626		−48.476	−50.102
BPK	m	0.457	0.404	0.529	0.508		0.532	0.578
	t_0 (d)	1.948	1.841	2.171	2.138		2.189	2.272
	μ_m (g L^{-1} d^{-1})	0.438	0.215	0.028	0.015		0.005	0.005
	k_{CA} (d^{-1})	0.355	0.441	0.256	0.277		0.251	0.210
	R^2	0.999	0.988	0.990	0.990		0.993	0.969
	RMSE	0.011	0.021	0.004	0.002		0.001	0.001
	NRMSE	0.874	4.254	3.745	3.940		3.209	6.542
	AIC	−32.242	−26.985	−39.908	−45.070		−55.522	−48.255
Second-order	k_{CA}" (L g^{-1} d^{-1})	1.322	5.093	7.914	18.071	45.701		26.412
	R^2	0.982	0.994	0.957	0.939	0.948		0.893
	RMSE	0.065	0.015	0.008	0.005	0.002		0.003
	NRMSE	5.237	3.067	7.693	9.590	8.476		12.189
	AIC	−19.914	−31.602	−36.148	−39.953	−49.751		−45.276
Cone	k_{CA} (d^{-1})	0.743	1.604	0.570	0.532	0.528		0.411
	n	2.218	1.306	1.840	2.787	2.078		2.455
	R^2	0.999	0.995	0.983	0.999	0.989		0.987
	RMSE	0.018	0.014	0.005	0.001	0.001		0.001
	NRMSE	1.465	2.841	4.783	1.375	3.877		4.253
	AIC	−28.106	−30.215	−37.949	−53.491	−54.008		−51.699
Modified Gompertz	μ_m (g L^{-1} d^{-1})	0.526	0.271	0.028	0.018	0.005		0.005
	λ (d)	0.274	0.276	0.016	0.373	0.115		0.115
	R^2	0.992	0.980	0.970	0.998	0.983		0.989
	RMSE	0.042	.027	0.007	0.001	0.001		0.001
	NRMSE	3.390	5.587	6.439	1.687	4.848		3.887
	AIC	−21.394	−24.805	−35.571	−51.854	−52.221		−52.420

Legend: k_{CA}: first-order CA production rate constant, k_{CA}": second-order CA production rate constant; n: form constant; λ: lag phase time; μ_m: maximum CA productivity; m: constant of the BPK model; R^2: coefficient of determination; RMSE: roof mean square error; NRMSE: normalized roof mean square error; AIC: Akaike Information Criteria.

(Monomolecular) estimated λ = 0.00 d. The form factor n of the Fitzhugh (n = 0.69 ± 0.33) and Cone (n = 1.91 ± 0.30) model indicates that there was a lag period related to CA production, although short (Table 7). Nevertheless, it can be concluded that the lag phase in relation to acid COD production from DW is quite short, which is desirable in biotechnological processes since the start-up time treating DW for product recovery would be small. Discrepancies between values may be related to the parameters used in each mathematical equation.

Another important parameter that has been estimated by the three models (Modified Gompertz, Logistic and BPK) is the maximum productivity rate (μ_m). The highest production rate was estimated by the BPK model (μ_m = 1.83 ± 0.28 gCOD L^{-1} d^{-1}), while the lowest was found by the Modified Gompertz model (μ_m = 0.98 ± 0.11 gCOD L^{-1} d^{-1}). The Logistic model provided intermediate productivity between the values estimated by the other two previous models (μ_m = 1.29 ± 0.18 gCOD L^{-1} d^{-1}).

The best models to simulate individual CA production from DW were: First-order model for HAc, HBu, and HVa; Second-order model for HPr; and Fitzhugh model for i-HVa and HCa (Table 8). There was a satisfactory visual adjustment of all models to the CA progression curve over time (Fig. 3), with an emphasis on the HAc curve (Fig. 3A), described optimally by the First-order model (R^2 = 0.999 and AIC = -34.242), and for the i-HVa curve (Fig. 3D), which was perfectly described by the Fitzhugh model (R^2 = 0.999 and AIC = -59.304).

Considering the models that best fit the experimental data, the first order product formation rate constant (k_{CA}), which could be estimated from both First-order and Fitzhugh models, was higher for i-HVa (k_{CA} = 0.748 d^{-1}, Fitzhugh model) and smaller for HVa (k_{CA} = 0.401 d^{-1}, First-order model). HAc, HBu, and HCa presented intermediate values, with k_{CA} equal to 0.611; 0.411 and 0.544 d^{-1}, respectively. Although CA production was characterized by first-order kinetics, the Second-order model was better adjusted to HPr production, and the second-order rate constant (k_{CA}") was 5.093 L g^{-1} d^{-1}. Such value cannot be directly compared with k_{CA} of the other acids because it has a different unit.

Maximum productivity rate (μ_m) could be estimated by three

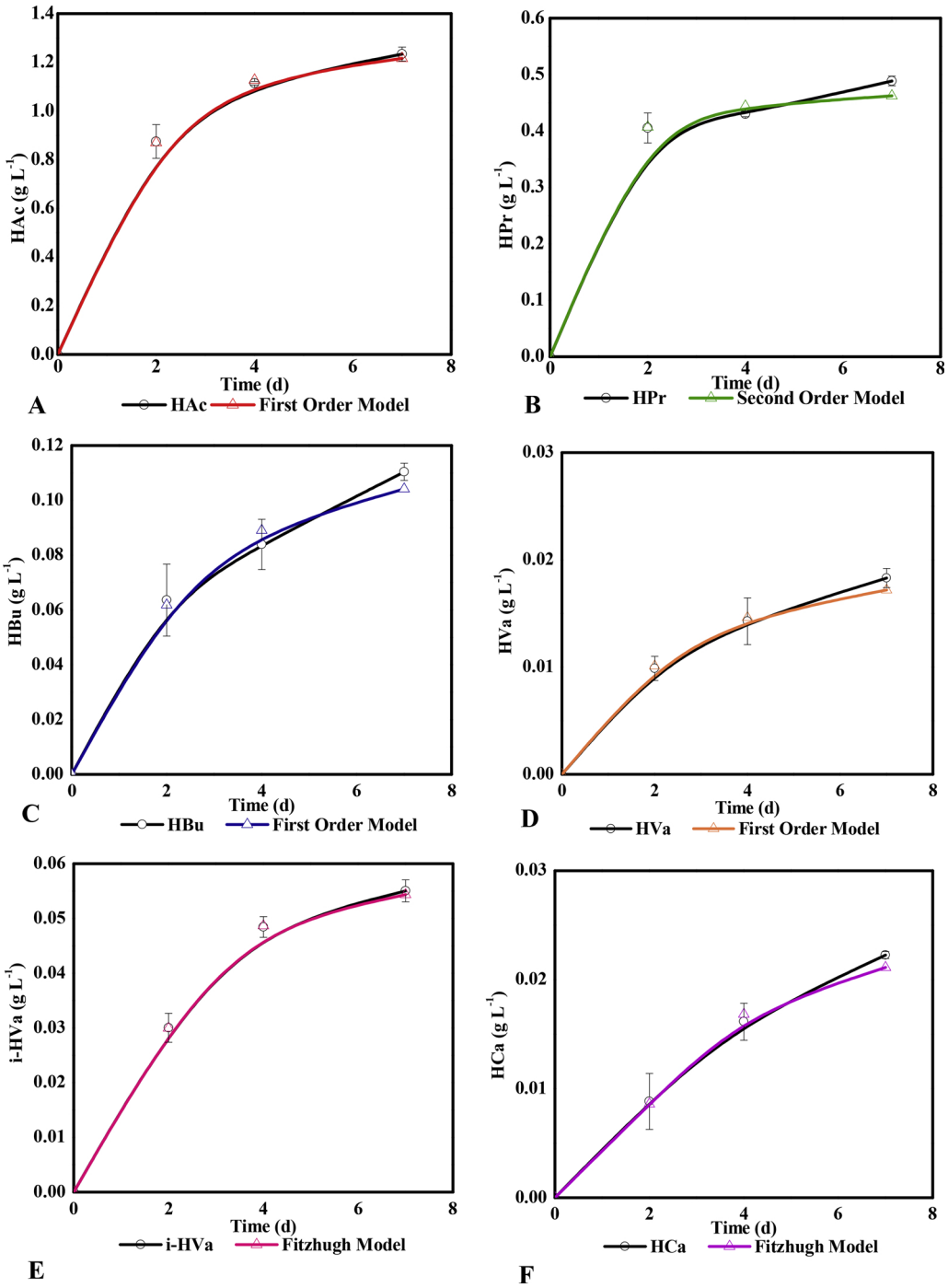

Fig. 3. Kinetic modeling of the individual production of carboxylic acids from the fermentative assays using dairy wastewater as substrate. A. HAc. B. HPr. C. HBu. D. i-HVa, E. HVa. F. HCa.

models (Modified Gompertz, Logistic and BPK). The values that most closely approximated to the real maximum productivity calculated from the concentration data obtained on the collection days (Table 5, Section 3.2) were, in mg L^{-1} d^{-1}, 438 (BPK model); 215 (BPK model); 28 (Modified Gompertz model); 15 (BPK model); 5 (BPK model) and 5 (BPK model), for HAc, HPr, HBu, i-HVa, HVa and HCa, respectively, and the BPK model estimated this parameter more satisfactorily. Lag phase lower than one day to start the production of all acids indicated that the microorganisms quickly used the substrate for CA production, as discussed for the production curve of acid in terms of COD (Fig. 2).

4. Conclusions

The tests showed that DW is a readily fermentable substrate to acidogenic microorganisms because it presents high rates of short-chain CA formation in the first two days of the experiment. The low concentrations of medium-chain CA found indicate that fats and proteins did not function as the main carbon source for DW fermentation. However, HCa was produced without the external addition of electron donors. The yield obtained was 0.66 mgCA $mgCOD_A^{-1}$, which corresponds to 0.83 $mgCOD_{CA}$ $mgCOD_A^{-1}$. Models that describe an exponential phase are the most suitable for the simulation of CA

production. Therefore, DW appears to be a high potential substrate for producing added-value products such as short-chain and medium-chain carboxylic acids.

Declaration of Competing Interests

The authors declare that they have no known competing financial interests or personal relationships that could have appeared to influence the work reported in this paper.

Author contribution statement

Milena Maciel Holanda Coelho: helped the experiments during the undergraduate studies on the Biotechnology Major at Federal University of Ceará.

Naassom Wagner Sales Morais: performed the experiments during his master´s study at the Civil Enginnering Program at the Federal University of Ceará.

Erlon Lopes Pereira: Assistant professor Federal University of Ceará and co-supervisor of the students.

Renato Carrhá Leitão: part of the analysis was performed at Embrapa and he helped in the experiment planning and discussion of the results.

André Bezerra dos Santos: was the supervisor of the students and leader of the Environmental Technology group at the Federal University of Ceará.

Acknowledgments

The authors would like to thank the support given by the following Brazilian institutions: National Council for Scientific and Technological Development – CNPq; Higher Education Personnel Improvement Coordination – CAPES; Minas Gerais State Research Support Foundation – FAPEMIG; National Institute of Science and Technology in Sustainable Sewage Treatment Stations – INCT Sustainable ETEs and Brazilian Agricultural Research Corporation -– EMBRAPA.

References

[1] I.O. Bolaji, D. Dionisi, Acidogenic fermentation of vegetable and salad waste for chemicals production: effect of pH buffer and retention time, J. Environ. Chem. Eng. 5 (2017) 5933–5943, https://doi.org/10.1016/j.jece.2017.11.001.

[2] R. Kleerebezem, B. Joosse, R. Rozendal, M.C.M. Van Loosdrecht, Anaerobic digestion without biogas? Rev. Environ. Sci. Biotechnol. 14 (2015) 787–880, https://doi.org/10.1007/s11157-015-9374-6.

[3] I.M. van Aarle, A. Perimenis, J. Lima-Ramos, E. de Hults, I.F. George, P.A. Gerin, Mixed inoculum origin and lignocellulosic substrate type both influence the production of volatile fatty acids during acidogenic fermentation, Biochem. Eng. J. 103 (2015) 242–249, https://doi.org/10.1016/j.bej.2015.07.016.

[4] S.K. Bhatia, Y.-H. Yang, Microbial production of volatile fatty acids: current status and future perspectives, Rev. Environ. Sci. Biotechnol. 16 (2017) 327–345, https://doi.org/10.1007/s11157-017-9431-4.

[5] W. Fang, X. Zhang, Z. Panyue, J. Wan, G. Hongxiao, D.S.M. Ghasimi, X.C. Morera, T. Zhang, Overview of key operation factors and strategies for improving fermentative volatile fatty acid production and product regulation from sewage sludge, J. Environ. Sci. (China). 87 (2020) 93–111, https://doi.org/10.1016/j.jes.2019.05.027.

[6] A.N. Kumar, S.V. Mohan, Acidogenesis of waste activated sludge — biohydrogen production with simultaneous short chain carboxylic acids, J. Environ. Chem. Eng. 6 (2018) 2983–2991, https://doi.org/10.1016/j.jece.2018.04.032.

[7] M. Zhou, B. Yan, J.W.C. Wong, Y. Zhang, Enhanced volatile fatty acids production from anaerobic fermentation of food waste: a mini-review focusing on acidogenic metabolic pathways, Bioresour. Technol. 248 (2018) 68–78, https://doi.org/10.1016/j.biortech.2017.06.121.

[8] Food and Agriculture Organization of The United Nations (FAO), Dairy Market Review, FAO, Roma, 2018 < http://www.fao.org/3/I9210EN/i9210en.pdf > . (Accessed April 15, 2019).

[9] T. Ahmad, R.M. Aadila, H. Ahmeda, U. Rahman, B.C.V. Soares, S.L. Souza, Q, T.C. Pimentel, H. Scudino, J.T. Guimarães, E.A. Esmerino, M.Q. Freitas, R.B. Almada, S.M.R. Vendramel, M.C. Silva, A.G. Cruz, Treatment and utilization of dairy industrial waste: a review, Trends Food Sci. Technol. 88 (2019) 361–372, https://doi.org/10.1016/j.tifs.2019.04.003.

[10] A.C. Bortoluzzi, J.A. Faitão, M.D. Luccio, R.M. Dallago, J. Ste, G.L. Zabot, M.V. Tres, Dairy wastewater treatment using integrated membrane systems, J. Environ. Chem. Eng. 5 (2017) 4819–4827, https://doi.org/10.1016/j.jece.2017.09.018.

[11] E. Daneshvar, M.J. Zarrinmehra, E. Koutrac, M. Kornarosc, O. Farhadianb, A. Bhatnagara, Sequential cultivation of microalgae in raw and recycled dairy wastewater: microalgal growth, wastewater treatment and biochemical composition, Bioresour. Technol. 273 (2019) 556–564, https://doi.org/10.1016/j.biortech.2018.11.059.

[12] B. Farizoglu, S. Uzuner, The investigation of dairy industry wastewater treatment in a biological high performance membrane system, Biochem. Eng. J. 57 (2011) 46–54.

[13] J.P. Kushwaha, V.C. Srivastava, I.D. Mall, Sequential batch reactor for dairy wastewater treatment: parametric optimization; kinetics and waste sludge disposal, J. Environ. Chem. Eng. 1 (2013) 1036–1043, https://doi.org/10.1016/j.jece.2013.08.018.

[14] M. Atasoy, I. Owusu-Agyeman, E. Plaza, Z. Cetecioglu, Bio-based volatile fatty acid production and recovery from waste streams: current status and future challenges, Bioresour. Technol. 268 (2018) 773–786, https://doi.org/10.1016/j.biortech.2018.07.042.

[15] I.M. Abu-Reesh, Kinetics of anaerobic digestion of labaneh whey in a batch reactor, African J. Biotechnol. 13 (2014) 1745–1755, https://doi.org/10.5897/ajb2013.13310.

[16] C. Jiménez-González, J.M. Woodley, Bioprocesses: Modeling needs for process evaluation and sustainability assessment, Comput. Chem. Eng. 34 (2010) 1009–1017, https://doi.org/10.1016/j.compchemeng.2010.03.010.

[17] C. Hu, B. Yan, K. Wang, X. Xiao, Modeling the performance of anaerobic digestion reactor by the anaerobic digestion system model (ADSM), J. Environ. Chem. Eng. 6 (2018) 2095–2104, https://doi.org/10.1016/j.jece.2018.03.018.

[18] N. Phukoetphim, A. Salakkam, P. Laopaiboon, L. Laopaiboon, Kinetic models for batch ethanol production from sweet sorghum juice under normal and high gravity fermentations: logistic and modified Gompertz models, J. Biotechnol. 243 (2017) 69–75, https://doi.org/10.1016/j.jbiotec.2016.12.012.

[19] A. Ware, N. Power, Modelling methane production kinetics of complex poultry slaughterhouse wastes using sigmoidal growth functions, Renew. Energy 104 (2017) 50–59, https://doi.org/10.1016/j.renene.2016.11.045.

[20] J.J. Murcia, M. Hernández-Laverde, H. Rojas, E. Muñoz, J.A. Navío, M.C. Hidalgo, Study of the effectiveness of the flocculation-photocatalysis in the treatment of wastewater coming from dairy industries, J. Photochem, Photobiol. A Chem. 358 (2018) 256–264, https://doi.org/10.1016/j.jphotochem.2018.03.034.

[21] R.I. Dams, M.B. Viana, A.A. Guilherme, C.M. Silva, A.B. dos Santos, L.T. Angenent, S.T. Santaella, R.C. Leitão, Production of medium-chain carboxylic acids by anaerobic fermentation of glycerol using a bioaugmented open culture, Biomass Bioenergy 118 (2018) 1–7, https://doi.org/10.1016/j.biombioe.2018.07.023.

[22] M.B. Viana, R.I. Dams, B.M. Pinheiro, R.C. Leitão, S.T. Santaella, A.B. dos Santos, The source of inoculum and the method of methanogenesis inhibition can affect biological hydrogen production from crude glycerol, Bioenergy Res. 12 (2019) 1–10, https://doi.org/10.1007/s12155-019-09994-5.

[23] APHA (American Public Health Association), American Water Works Association, Water environment Federation, Standard Methods for the Examination of Water and Wastewater, 22th ed., American Public Health Association (APHA), American Water Works Association and Water Environment Federation, Washington, DC, 2012.

[24] R. Moscoviz, E. Trably, N. Bernet, H. Carrère, The environmental biorefinery: state-of-the-art on the production of hydrogen and value-added biomolecules in mixed-culture fermentation, Green Chem. 20 (2018) 3159–3179, https://doi.org/10.1039/c8gc00572a.

[25] H. Akaike, Information theory and an extension of the maximum likelihood principle, Selected Papers of Hirotugu Akaike, first ed., Springer, New York, 1998.

[26] D.R.S. Lima, O.F.H. Adarme, B.E.L. Baêta, L.V.A. Gurgel, S.F. de Aquino, Influence of different thermal pretreatments and inoculum selection on the biomethanation of sugarcane bagasse by solid-state anaerobic digestion: a kinetic analysis, Ind. Crops Prod. 111 (2018) 684–693, https://doi.org/10.1016/j.indcrop.2017.11.048.

[27] F.C. Silva, L.S. Serafim, H. Nadais, L. Arroja, I. Capela, Acidogenic fermentation towards valorisation of organic waste streams into volatile fatty acids, Chem. Biochem. Eng. Q. 27 (2013) 467–476.

[28] V.H. Grisales Díaz, M.J. Willis, Ethanol production using Zymomonas mobilis: development of a kinetic model describing glucose and xylose co-fermentation, Biomass Bioenergy 123 (2019) 41–50, https://doi.org/10.1016/j.biombioe.2019.02.004.

[29] L. Hao, L. Fan, L. Li, L. Shao, P. He, Response of anaerobes to methyl fluoride, 2-bromoethanesulfonate and hydrogen during acetate degradation, J. Environ. Sci. China (China) 25 (2013) 857–864, https://doi.org/10.1016/S1001-0742(12)60203-4.

[30] J. Jiang, Y. Zhang, K. Li, Q. Wang, C. Gong, M. Li, Volatile fatty acids production from food waste: effects of pH, temperature, and organic loading rate, Bioresour. Technol. 143 (2013) 525–530, https://doi.org/10.1016/j.biortech.2013.06.025.

[31] L.T. Angenent, H. Richter, W. Buckel, C.M. Spirito, K.J.J. Steinbusch, C.M. Plugge, D.P.B.T.B. Strik, T.I.M. Grootscholten, C.J.N. Buisman, H.V.M. Hamelers, Chain elongation with reactor microbiomes: open-culture biotechnology to produce biochemicals, Environ. Sci. Technol. 50 (2016) 2796–2810, https://doi.org/10.1021/acs.est.5b04847.

[32] Q. Wu, X. Bao, W. Guo, B. Wang, Y. Li, H. Luo, H. Wang, N. Ren, Medium chain carboxylic acids production from waste biomass: current advances and perspectives, Biotechnol. Adv. 37 (2019) 1–17, https://doi.org/10.1016/j.biotechadv.2019.03.003.

[33] A.N. Da Silva, W.V. Macêdo, I.K. Sakamoto, D.L.A.D. Pereyra, C.O. Mendes, S.I. Maintinguer, R.A. Caffaro Filho, M.H.Z. Damianovic, M.B.A. Varesche, E.L.C. De Amorim, Biohydrogen production from dairy industry wastewater in an anaerobic

fluidized-bed reactor, Biomass Bioenergy 120 (2019) 257–264, https://doi.org/10.1016/j.biombioe.2018.11.025.
[34] J. Garcia-Aguirre, E. Aymerich, G. González-Mtnez. de J., M. Esteban-Gutiérrez, Selective VFA production potential from organic waste streams: assessing temperature and pH influence, Bioresour. Technol. 244 (2017) 1081–1088, https://doi.org/10.1016/j.biortech.2017.07.187.
[35] J. Yin, X. Yu, K. Wang, D. Shen, Acidogenic fermentation of the main substrates of food waste to produce volatile fatty acids, Int. J. Hydrogen Energy 41 (2016) 21713–21720, https://doi.org/10.1016/j.ijhydene.2016.07.094.
[36] M. Chartrain, J.G. Zeikus, Microbial ecophysiology of whey biomethanation: intermediary metabolism of lactose degradation in continuous culture, Appl. Environ. Microbiol. 51 (1986) 180–187.
[37] G. Strazzera, F. Battista, N.H. Garcia, N. Frison, D. Bolzonella, Volatile fatty acids production from food wastes for biorefinery platforms: a review, J. Environ. Manage. 226 (2018) 278–288, https://doi.org/10.1016/j.jenvman.2018.08.039.
[38] A.N. Hassan, B.K. Nelson, Invited review: anaerobic fermentation of dairy food wastewater, J. Dairy Sci. 95 (2012) 6188–6203, https://doi.org/10.3168/jds.2012-5732.
[39] R. Chandra, C. Castillo-Zacarias, P. Delgado, R. Parra-Saldívar, A biorefinery approach for dairy wastewater treatment and product recovery towards establishing a biorefinery complexity index, J. Clean. Prod. 183 (2018) 1184–1196, https://doi.org/10.1016/j.jclepro.2018.02.124.
[40] W.S. Kisaalita, K.L. Pinder, K.V. Lo, Acidogenic fermentation of lactose, Biotechnol. Bioeng. 30 (1987) 88–95, https://doi.org/10.1002/bit.260300113.
[41] D. Shen, J. Yin, X. Yu, M. Wang, Y. Long, J. Shentu, T. Chen, Acidogenic fermentation characteristics of different types of protein-rich substrates in food waste to produce volatile fatty acids, Bioresour. Technol. 227 (2017) 125–132, https://doi.org/10.1016/j.biortech.2016.12.048.
[42] N. Bermúdez-Penabad, C. Kennes, M.C. Veiga, Anaerobic digestion of tuna waste for the production of volatile fatty acids, Waste Manag. 68 (2017) 96–102, https://doi.org/10.1016/j.wasman.2017.06.010.
[43] H.G. Yu, H.H. Fang, Acidogenesis of dairy wastewater at various pH levels, Water Sci. Technol. 45 (2002) 201–206.
[44] S. Bengtsson, J. Hallquist, A. Werker, T. Welander, Acidogenic fermentation of industrial wastewaters: effects of chemostat retention time and pH on volatile fatty acids production, Biochem. Eng. J. 40 (2008) 492–499, https://doi.org/10.1016/j.bej.2008.02.004.
[45] L. Feng, Y. Yan, Y. Chen, Kinetic analysis of waste activated sludge hydrolysis and short-chain fatty acids production at pH 10, J. Environ. Sci. China (China) 21 (2009) 589–594, https://doi.org/10.1016/S1001-0742(08)62312-8.
[46] N. Kythreotou, G. Florides, S.A. Tassou, A review of simple to scientific models for anaerobic digestion, Renew. Energy 71 (2014) 701–714, https://doi.org/10.1016/j.renene.2014.05.055.
[47] M.D. Putra, A.E. Abasaeed, A more generalized kinetic model for binary substrates fermentations, Process Biochem. 75 (2018) 31–38, https://doi.org/10.1016/j.procbio.2018.09.